Proceedings of OMAE 2007
26th International Conference on Offshore Mechanics and Arctic Engineering
San Diego, California, USA, June 10-15, 2007

OMAE2007-29073

EXPECTED SHAPE OF EXTREME WAVES IN STORM SEAS

M. Aziz Tayfun
College of Engineering & Petroleum, Kuwait University, Kuwait.
aziztayfun@usa.net

Francesco Fedele
School of Civil & Environmental Engineering, Georgia Institute of Technology, 210 Technology Circle, Savannah, Georgia 31407, USA

ABSTRACT

The theoretical expected structure of large nonlinear waves can be described, using the Gram-Charlier approximations of Jensen et al. (1995) and Jensen (1996, 2005), and the quasi-deterministic model of Fedele & Arena (2005). The second-order narrow-band approximation offers a simpler alternative to these models, as recently suggested in Tayfun & Fedele (2006). Herein, this latter alternative is elaborated further, deriving theoretical expressions for predicting the expected shape of large waves, conditional on somewhat more general constraints than those previously considered. The theoretical results are verified favorably with oceanic measurements gathered at deep and transitional water depths in the North Sea. Some comparisons of the present model with those of Jensen et al. (1995) and Fedele & Arena (2005) are also given, showing that all three models do in fact reasonably well in representing the expected profile of large waves in storm seas.

INTRODUCTION

The expected configuration of the nonlinear sea surface over the region of large waves in extreme seas has been of increasing practical and theoretical interest in recent years (see e.g. Fedele & Arena 2005; Fedele & Tayfun 2006; Guedes Soares & Pascoal 2005; Jensen et al. 1995; Jensen 1996, 2005; Petrova et al. 2006; Socquet-Juglard et al. 2005; Tayfun & Fedele 2007). In the linear Gaussian case, the conditional expected shapes of large waves are predicted well by the linear models devised by Lindgren (1972), Boccotti (2000), and Phillips et al. (1993). Although the formulations and constraints used in deriving these models differ somewhat, particularly in Phillips et al. (1993), it appears that they all yield essentially the same description for the conditional expected shape of large linear waves.

The conditional expected shape of large waves in second-order nonlinear seas has been considered more recently by Jensen et al. (1995) and Jensen (1996, 2005), using approximations based on the Edgeworth form of Gram-Charlier series, and by Fedele & Arena (2005), who generalized and extended the linear quasi-deterministic theories (QD 1) of Lindgren (1972) and Boccotti (2000) to second-order seas. The Fedele-Arena model (QD 2) satisfies the second-order Stokes wave theory exactly. So, it would seem that it should be a more accurate representation for the expected structure of large waves and wave groups than those derived from the Gram-Charlier type approximations. But, there have been no comparisons to show if that is really the case. Jensen's 1995 and 2005 models are essentially the same and also more elaborate than the earlier Jensen et al. (1995) model. However, comparisons demonstrate that the differences between these models tend to diminish for large waves (see e.g. Jensen 1996).

A simpler alternative to the Jensen et al. (1995), Jensen (1996, 2005) and Fedele-Arena QD 2 models is offered by the narrow-band (NB) model (Tayfun 1980, 1986). The NB model appears to be quite effective in describing the probability structure of the sea surface and its various extremal features, particularly, over the region of large waves (Socquet-Juglard et al. 2005; Tayfun 2006; Tayfun & Fedele 2007). Herein, the same model is elaborated further, following Tayfun & Fedele (2006), to develop a third model and theoretical expressions for describing the conditional expected shape of large waves in storm seas under more general conditions than those considered in the previous second-order models. These are verified with two different sets of oceanic data collected at deep and transitional water depths in the North Sea, and also with comparisons to the 1995 Jensen et al. (J) model, QD 1 models of Lindgren (1972), Boccotti (2000) and Phillips et al. (1993), and the QD 2 model of Fedele & Arena (2005).

MODEL, DEFINITIONS & PROBABILITY STRUCTURE

The zero-mean free surface elevation measured at a fixed point in time t and scaled with by its *rms* value, say, σ is approximated as

$$\eta = \eta_1 + \eta_2 = r\cos\chi + \frac{\mu}{2} r^2 \cos 2\chi = \eta_1 + \frac{\mu}{2}(\eta_1^2 - \hat{\eta}_1^2), \quad (1)$$

where $\eta_1 = r\cos\chi$ and $\hat{\eta}_1 = r\sin\chi$ describe, respectively, the first-order Gaussian profile and its Hilbert transform exactly; η_2 is the second-order correction to η for long-crested seas correct to $O(\nu^0)$, with $\nu = [m_0\, m_2 / m_1^2 - 1]^{1/2} \equiv$ spectral bandwidth, and $m_j \equiv j$-th ordinary moment of the spectral density $S_1(\omega)$ of η_1 as a function of circular frequency ω; $r(t) = [\eta_1^2 + \hat{\eta}_1^2]^{1/2} \equiv$ Rayleigh-distributed random amplitude of η_1, scaled with $\sigma = m_0^{1/2}$; $\chi = \tan^{-1}(\hat{\eta}_1 / \eta_1) \equiv$ random wave-phase, independent of r and uniformly distributed in $(0, 2\pi)$; and, $\mu = \sigma k_m = \sigma \omega_m^2 / g \equiv$ steepness parameter = *rms* surface slope of η_1, with $g = 9.8$ m/s^2 and $\omega_m = m_1 / m_0$. Further,

$$\lambda_3 = \langle \eta^3 \rangle = 3\langle \eta_1^2 \eta_2 \rangle = 3\mu \tag{2}$$

yields the skewness coefficient of η, correct to $O(\mu)$, as an upper bound to the observational values of $\lambda_3 = \langle \eta^3 \rangle$ in directional seas under deep-water conditions (Tayfun 2006). Using μ as an ordering parameter, η_1 is $O(1)$ whereas η_2 is $O(\mu)$. Thus, $\langle \eta_1^2 \rangle = \langle \hat{\eta}_1^2 \rangle = 1$ and $\langle \eta_1\, \eta_2 \rangle = 0$. All this suggests that the *rms* values, spectral densities, associated moments m_j, and the normalized auto- and cross-correlation kernels of η are the same as those of η_1, correct to $O(\mu)$.

The first-order variables η_1 and $\hat{\eta}_1$ are independent Gaussian, and the total wave-phase function can also be rewritten as $\chi = \omega_m t + \phi$, where $\phi(t) \equiv$ wave-phase function, uniformly distributed in $(0, 2\pi)$. Both derivatives $\dot{r} = \partial r / \partial t$ and $\dot{\phi} = \partial \phi / \partial t$ are $O(\nu)$ (Tayfun 1986). Assuming that the higher-order derivatives $\ddot{r}$ and $\ddot{\phi}$ are $O(\nu^2)$, then at wave crests or maxima of η_1, $\cos\chi = 1 + O(\nu^2)$, $\sin\chi = 0 + O(\nu)$, $\hat{\eta}_1 = 0 + O(\nu)$, $\dot{\eta}_1 = 0 + O(\nu)$, and $\ddot{\eta}_1 = -r\omega_m^2 + O(\nu^2) < 0$. Thus, $max\{\eta_1\} = r + O(\nu^2)$. However, because η_2 is an NB representation correct to $O(1)$, $max\{\eta_2\} = \mu\, r^2 / 2 + O(\nu)$. As a result, the maxima or crests of η are given by

$$max\{\eta\} \equiv y = r + \frac{1}{2}\mu\, r^2 + O(\nu). \tag{3}$$

An immediate implication of all these is that at the crests of η_1, the marginal probability densities (p.d.) of $\hat{\eta}_1$ and $\dot{\eta}$, conditional on $\eta_1 = r$, are both given by $\delta(0)$ to $O(1)$, whereas the p.d. of $\ddot{\eta}_1$ under the same condition is $\delta(\ddot{\eta}_1 + r\omega_m^2)$. Similarly, at the crests y of η, the p.d. of $\dot{\eta}$, conditional on $\eta_1 = r$ or $\eta = y$, is also $\delta(0)$ to $O(1)$, and the p.d. of $\ddot{\eta}$ takes the form $\delta(\ddot{\eta} + r\,\omega_m^2[1 + 2\mu r])$. Thus, given $\eta_1 = r$ or $\eta = y$, $\hat{\eta}_1$, $\dot{\eta}_1$ and $\dot{\eta}$ are zero, and $\ddot{\eta}_1$ and $\ddot{\eta}$ are always negative with probability 1 for the NB model. These are consistent with the conditions for the occurrence of maxima or wave crests, as they should be.

The p.d. and exceedance distribution (e.d.) of r are

$$p_r = r\exp(-r^2/2) \quad , \quad E_r = \exp(-r^2/2) \ , \tag{4}$$

where $r \geq 0$. Thus, the p.d. and e.d. of y can be expressed, respectively, as

$$p_y = \frac{p_r}{1 + \mu r} \quad , \quad E_y = E_r \ ; \quad y = r + \frac{1}{2}\mu\, r^2 . \tag{5}$$

The preceding expressions can be used to develop the mean of *y*, conditional on the threshold value $y_n = E_y^{-1}(1/n)$ for $n \geq 1$ corresponding to the largest (100 / *n*) % of wave crests, as in Tayfun (2006), viz.

$$y_{1/n} \equiv \langle\, y \,|\, y > y_n \,\rangle = r_{1/n} + \mu[1 + \ln(n)] \ , \tag{6a}$$

$$y_n = r_n + \frac{\mu}{2} r_n^2 , \tag{6b}$$

$$r_{1/n} = \langle\, r \mid r > r_n \,\rangle = r_n + \sqrt{\frac{\pi}{2}}\; n\; erfc\left(\frac{r_n}{\sqrt{2}}\right), \tag{6c}$$

$$r_n = \sqrt{2\ln(n)} = E_r^{-1}\left(\frac{1}{n}\right). \tag{6d}$$

where *erfc* stands for the complementary error function. Clearly, Eq. (6a) reduces to $r_{1/n}$ appropriate to linear narrow-band wave crests if $\mu = 0$. Further, let $\langle R_N \rangle$ and $\langle Y_N \rangle$ represent the mean largest wave crests in *N* linear and nonlinear waves, respectively. These have the forms (see. e.g. Tayfun 2004)

$$\langle R_N \rangle = \sqrt{2\ln(N)} + \frac{0.577216}{\sqrt{2\ln(N)}} \ , \tag{7a}$$

$$\langle Y_N \rangle = \langle R_N \rangle + \mu\, [\, 0.577216 + \ln(N)\,] \ . \tag{7b}$$

For simplicity, let $\xi_1 = \eta_1(t)$, $\xi_2 = \eta_1(t+\tau)$, $\hat{\xi}_1 = \hat{\eta}_1(t)$ and $\hat{\xi}_2 = \hat{\eta}_1(t+\tau)$. On this basis,

$$\rho(\tau) = \langle \xi_1 \xi_2 \rangle = \langle \hat{\xi}_1 \hat{\xi}_2 \rangle = \int S(\omega) \cos \omega \, d\omega \,, \tag{8a}$$

$$\hat{\rho}(\tau) = \langle \xi_1 \hat{\xi}_2 \rangle = \langle \hat{\xi}_1 \xi_2 \rangle = \int S(\omega) \sin \omega \, d\omega \,. \tag{8b}$$

The conditional p.d. of ξ_2, given ξ_1, is

$$p_{\xi_2|\xi_1}(x \,|\, \xi_1) = \frac{1}{\sqrt{2\pi(1-\rho^2)}} \exp\left[-\frac{(x-\rho\,\xi_1)^2}{2(1-\rho^2)} \right] . \tag{9}$$

The conditional p.d. of $\hat{\xi}_2$, given $\hat{\xi}_1$ is exactly the same as Eq. (9), but the p.d. of $\hat{\xi}_2$, conditional on ξ_1, has the form

$$p_{\hat{\xi}_2|\xi_1}(x|\xi_1) = \frac{1}{\sqrt{2\pi(1-\hat{\rho}^2)}} \exp\left[-\frac{(x-\hat{\rho}\,\xi_1)^2}{2(1-\hat{\rho}^2)} \right] . \tag{10}$$

EXPECTED SHAPE OF NB NONLINEAR WAVES

Consider Eq. (1), let $\zeta_1 = \eta(t)$, $\zeta_2 = \eta(t+\tau)$, and define the events $a \equiv \{\zeta_1 = \gamma\}$ and $a_1 \equiv \{\xi_1 = \gamma_1\}$. On this basis,

$$\langle \zeta_2 \mid a \rangle = \langle \xi_2 \mid a_1 \rangle + \frac{\mu}{2} \left(\langle \xi_2^2 \mid a_1 \rangle - \langle \hat{\xi}_2^2 \mid a_1 \rangle \right), \tag{11}$$

where, from Eqs. (9) and (10), $\langle \xi_2 | \xi_1 = \gamma_1 \rangle = \gamma_1 \rho$; $\langle \xi_2^2 \mid a_1 \rangle = 1 + \rho^2(\gamma_1^2 - 1)$; and, $\langle \hat{\xi}_2^2 \mid a_1 \rangle = 1 + \hat{\rho}^2(\gamma_1^2 - 1)$. Since $\zeta_2 = \eta(t+\tau)$ and $a \equiv \{\eta(t) = \gamma\}$, these simplify Eq. (11) to

$$\langle \eta(t+\tau) \mid \eta(t) = \gamma \rangle = \gamma_1 \rho + \frac{\mu}{2} (\gamma_1^2 - 1)(\rho^2 - \hat{\rho}^2) . \tag{12}$$

For $\gamma_1^2 >> 1$, the preceding expression reduces to

$$\langle \eta(t+\tau) \mid \eta(t) = \gamma \rangle \approx \gamma_1 \rho + \frac{\mu}{2} \gamma_1^2 (\rho^2 - \hat{\rho}^2) . \tag{13}$$

At $\tau = 0$, $\langle \eta(t) \mid \eta(t) = \gamma \rangle = \gamma$, $\rho(0) = 1$, $\hat{\rho}(0) = 0$. Thus,

$$\gamma \approx \gamma_1 + \frac{\mu}{2} \gamma_1^2 \,, \tag{14a}$$

$$\gamma_1 \approx (-1 + \sqrt{1 + 2\mu\gamma}) / \mu \,. \tag{14b}$$

These results also follow from Eq. (1) directly by taking the conditional expected values, given $\eta(t) = \gamma$ and $\eta_1(t) = \gamma_1$. So, Eq. (13) is theoretically more consistent than Eq. (12) with the NB approximations assumed in Eq. (1), and thus with the conditional p.d. $\delta(0)$ of $\hat{\eta}_1(t+\tau)$ as $\tau \to 0$, given $\eta_1(t) = \gamma_1$, as discussed before. Evidently, setting $\mu = 0$ in Eq. (13) reduces it identically to the QD 1 model in Lindgren (1972) and Boccotti (1989, 2000).

The relative simplicity of the NB model allows derivations of the expected shapes of large waves, conditional on different type of constraints. For example, consider $\langle \zeta_2 \mid \zeta_1 > \gamma \rangle$. Defining the events $A \equiv \{\zeta_1 > \gamma\}$ and $A_1 \equiv \{\xi_1 > \gamma_1\}$, it is immediate from Eq. (1) that

$$\langle \zeta_2 \mid A \rangle = \langle \xi_2 \mid A_1 \rangle + \frac{1}{2} \mu \left(\langle \xi_2^2 \mid A_1 \rangle - \langle \hat{\xi}_2^2 \mid A_1 \rangle \right) . \tag{15}$$

Using Eqs. (9) and (10),

$$p_{\xi_2|A_1}(x|A_1) = \frac{\exp(-x^2/2)}{Q(\gamma_1)\,\pi\sqrt{2}} \int_{u_0}^{\infty} \exp(-u^2)\, du \,, \tag{16a}$$

$$p_{\hat{\xi}_2|A_1}(x|A_1) = \frac{\exp(-x^2/2)}{Q(\gamma_1)\,\pi\sqrt{2}} \int_{\hat{u}_0}^{\infty} \exp(-u^2)\, du \,, \tag{16b}$$

where

$$Q(\gamma_1) = \Pr\{A_1\} = erfc(\gamma_1/\sqrt{2})/2 \,, \tag{17a}$$

$$u_0 = (\gamma_1 - x\rho)/\sqrt{2\,(1-\rho^2)} \,, \tag{17b}$$

$$\hat{u}_0 = (\gamma_1 - x\hat{\rho})/\sqrt{2\,(1-\hat{\rho}^2)} \,. \tag{17c}$$

Thus, $\langle \xi_2 \mid A_1 \rangle = C\rho$, $\langle \xi_2^2 \mid A_1 \rangle = 1 + C\gamma_1\rho^2$, and $\langle \hat{\xi}_2^2 \mid A_1 \rangle = 1 + C\gamma_1\hat{\rho}^2$, with

$$C = C(\gamma_1) = \sqrt{\frac{2}{\pi}} \frac{\exp(-\gamma_1^2/2)}{erfc(\gamma_1/\sqrt{2})} \,. \tag{18}$$

As a result, Eq. (15) can be expressed in the form

$$\langle \eta(t+\tau) \mid \eta(t) > \gamma \rangle = C(\gamma_1)[\rho + \frac{\mu}{2}\gamma_1(\rho^2 - \hat{\rho}^2)] \,. \tag{19}$$

As $\tau \to 0$, this expression leads to

$$\langle \eta(t) \mid \eta(t) > \gamma \rangle \equiv \beta(\gamma) = (1 + \frac{\mu}{2}\gamma_1)\, C(\gamma_1) . \tag{20}$$

Given μ and β, γ_1 follows via successive substitutions from

$$z_{i+1} = \beta \frac{z_i}{C(z_i)} \left(1 + \frac{\mu}{2} z_i \right)^{-1} , \qquad (21)$$

where $i = 0, 1, 2, \ldots$ and $z_0 = \beta$.

As $\mu \to 0$, Eq. (19) reduces to the QD 1 model in Phillips et al. (1993a). In either case, it is tempting to use the expansion $C(\gamma_1)/\gamma_1 = 1 - \gamma_1^{-2} + \cdots$, and thus set $C(\gamma_1) \cong \gamma_1$ for $\gamma_1^2 >> 1$. But, this approximation really requires unrealistically large values of γ_1 for it to differ negligibly, say, e.g. by less than 1-2 %, from the exact form of $C(\gamma_1)$, as shown in the upper part of Fig. 1 below.

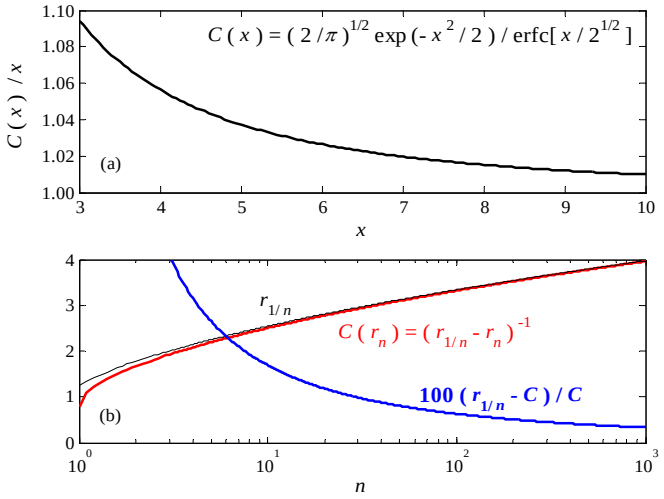

Fig. 1. (a) Asymptotic behavior of $C(x)/x$ versus x. (b) $C(r_n)$ in comparison with $r_{1/n}$ and % error in $C(r_n) \cong r_{1/n}$.

In practice, γ and β need to be estimated via wave-by-wave analysis from observational data, for example, for the largest $(100/n)$ % wave crests. Clearly, this would correspond to an empirical or data-dependent application of the NB model, hereafter referred to as NB-data. If the surface spectral density is given, then a simpler alternative and one that should be preferable to the NB-data model of Eqs. (19)-(21) is to implement it in a data-independent predictive mode, by replacing β, γ, γ_1 and C in Eq. (19) with their theoretical values, viz. $\beta = y_{1/n}$, $\gamma = y_n$, $\gamma_1 = r_n$ and $C(r_n) = (r_{1/n} - r_n)^{-1}$. Further, setting $C(r_n) \cong r_{1/n}$ causes errors less than 2 % when $n \geq 10$, as shown in the lower part of Fig. 1. All these simplify Eq. (19) to

$$\langle \eta(t+\tau) \,|\, \eta(t) > y_n \rangle = r_{1/n} \left[\rho + \frac{\mu}{2} r_n (\rho^2 - \hat{\rho}^2) \right] , \qquad (22)$$

hereafter referred to as NB-theory.

A further application of NB-theory via Eq. (13) would be to predict the expected profile of the largest wave in N waves. This would simply require setting $\gamma_1 = \langle R_N \rangle$ and $\gamma = \langle Y_N \rangle$ from Eqs. (7b) and (7b), respectively.

Finally, it is worthwhile to mention that the NB model and its fairly simple probability structure would easily allow for the formulation of the theoretically expected shape of large waves conditional on other types of constraints. These include, for example, $\langle \eta(t+\tau) \,|\, \gamma_a < \eta(t) \leq \gamma_b \rangle$ and possible others, but they will not pursued here due to limited space.

JENSEN et al. (J) & FEDELE-ARENA (QD 2) MODELS

Jensen et al. (1995) consider second-order nonlinear sea surfaces, approximating the p.d. of $\eta(t+\tau)$, given $\eta(t) = \gamma$ at a maximum or wave crest, in terms of Gram-Charlier series. The resulting model (J) is of the form

$$\langle \eta(t+\tau) \,|\, \eta(t) = \gamma \rangle = \gamma \rho + \frac{1}{2} (\gamma^2 - 1)(\lambda_{21} - \lambda_3 \rho) , \qquad (23)$$

where $\lambda_{21} = \langle \eta^2(t+\tau) \eta(t) \rangle$.

The QD 2 model of Fedele & Arena (2005) generalizes the linear quasi-deterministic models of Lindgren (1972) and Boccotti (1989) to derive the second-order conditional expected shape of $\eta(t+\tau)$, given $\eta(t) = \gamma$ and $\gamma >> 1$. This result can be expressed as

$$\langle \eta(t+\tau) \,|\, \eta(t) = \gamma \rangle = \gamma_1 \rho + \frac{1}{6} \gamma_1^2 \lambda , \qquad (24)$$

where (Tayfun 2006; Tayfun & Fedele 2007)

$$\begin{aligned} \lambda(\tau) &= 3 \langle \eta_1^2(t) \, \eta(t+\tau) \rangle \\ &= \frac{3}{2} \iint [K^+ \cos \Phi^+ + K^- \cos \Phi^-] \, \Psi(\boldsymbol{k}) \Psi(\boldsymbol{k}') \, d\boldsymbol{k} \, d\boldsymbol{k}' , \end{aligned} \qquad (25)$$

with $\boldsymbol{k} \equiv$ wave-number vector, $\Psi \equiv$ wave-number spectral density, $\Phi^{\pm} = (\omega \pm \omega')\tau$, and $K^{\pm} \equiv$ second-order interaction kernels (Sharma & Dean 1979). Now, first note that $\lambda(\tau) \leq \lambda(0) = 3 \langle \eta_1^2 \, \eta \rangle = \langle \eta^3 \rangle = \lambda_3$ and $0 < \lambda_3 < 3\mu$ in the most general case (Tayfun 2006). More significantly, QD 2 is consistent with the second-order theory under general conditions for directional seas at deep and transitional water depths. Setting $\tau = 0$ and $\mu_a = \lambda(0)/3$ in Eq. (24) will lead to

$$\gamma_1 = (-1 + \sqrt{1 + 2 \mu_a \gamma}) / \mu_a . \qquad (26)$$

This result has the same form as Eq. (14b), but $\mu_a < \mu$ since $\lambda_3 = \lambda(0) = 3\mu_a < 3\mu$ in the most general case. Nonetheless, as $\nu \to 0$, then $\lambda_3 \to 3\mu$ and so $\mu_a \to \mu$ as an upper bound. In the latter case, NB and QD 2 models both lead to the same representation for second-order wave crests and troughs.

The formulations of J and QD 2 models do not include the conditional expected shape of large waves under different constraints. In particular, formulating $\langle \eta(t+\tau) \mid \eta(t) > \gamma \rangle$ via Jensen's approach can require rather cumbersome algebra. In contrast, the same formulation via the QD theory is surprisingly easy. To elaborate this, compare the Phillips et al. (1993) type QD 1 model for $\gamma_1 >> 1$, viz.,

$$\langle \eta_1(t+\tau) \mid \eta_1(t) > \gamma_1 \rangle = C(\gamma_1) \int \Psi(\boldsymbol{k}) \cos \omega\tau \, d\boldsymbol{k} \qquad (27)$$

with the random spectral representation

$$\eta_1(t) = \int \cos[\omega t + \varepsilon(\boldsymbol{k})] \, dZ(\boldsymbol{k}) \,, \qquad (28)$$

where $\varepsilon(\boldsymbol{k}) \equiv$ independent random phases distributed uniformly in $(0, 2\pi)$, and $dZ(\boldsymbol{k}) =$ random amplitudes with orthogonal increments such that $\langle | dZ(\boldsymbol{k}) |^2 \rangle = \Psi(\boldsymbol{k}) \, d\boldsymbol{k}$. Evidently, QD 1 is fully consistent with the first-order equations of wave motion since it has the same functional representation as η_1 except that the random phases are all set to 0, and the random amplitudes $dZ(\boldsymbol{k})$ are replaced with $C(\gamma_1)\Psi(\boldsymbol{k}) \, d\boldsymbol{k}$. Proceeding further, the second-order correction η_2 to η_1 is of the form

$$\eta_2 = (1/4) \iint [K^+ \cos \Omega^+ + K^- \cos \Omega^-] \, dZ(\mathbf{k}) \, dZ(\mathbf{k}') \,, \quad (29)$$

where $\Omega^{\pm} = (\omega \pm \omega')t + \varepsilon(\boldsymbol{k}) \pm \varepsilon(\boldsymbol{k}')$. The latter expression with all phases set to 0 and $dZ(\boldsymbol{k})$ replaced by $C(\gamma_1)\Psi(\boldsymbol{k}) \, d\boldsymbol{k}$ likewise satisfies the second-order equations of wave motion, thus leading to the QD 2 form given simply by

$$\langle \eta(t+\tau) \mid \eta(t) > \gamma \rangle = C(\gamma_1)[\, \rho + \frac{1}{6} \, C(\gamma_1) \, \lambda(\tau) \,] \,. \quad (30)$$

As in the case of the NB model, the QD 2 models of Eqs. (24) and (30) can be applied either as data-dependent models or in a data-independent predictive mode, given the surface spectral density. The predictive mode of QD 2 will henceforth be referred to as QD 2-theory. In using Eq. (30) in the latter case, the empirical parameters are replaced by their theoretical values from Eqs. (6a)-(6d) corresponding to $\mu = \mu_a$, viz. $y_{1/n} \equiv \langle \eta(t+\tau) \mid \eta(t) > \gamma \rangle$, $\gamma \equiv y_n$, and $C(\gamma_1) \cong r_{1/n}$ to predict the expected profile of the largest $(100/n)$ % wave crests. Similarly, for the expected profile of the largest in *N* waves, it suffices to use QD 2 form of Eq. (24), setting in this case $\mu = \mu_a$, $\gamma_1 = \langle R_N \rangle$ and $\gamma = \langle Y_N \rangle$ from Eqs. (7a) and (7b), respectively.

In theory, the NB model describes long-crested waves. Its potential usefulness in describing short-crested waves has not so far been tested fully. Clearly, the first-order NB component is valid for such waves under general conditions. And, the long-crestedness constraint is inherent in approximating the second-order nonlinear effects due to bound modes arising from the frequency-sum terms of the first-order field, correct to $O(\nu^0)$ only. In practice, however, oceanic data seem to suggest that relatively large waves often display features associated with long-crested waves locally, behaving as slowly varying Stokian waves with essentially no secondary crests or troughs, unlike short-crested wider-band waves. So, this may at least partially explain the relative success of the second-order NB model in predicting large surface elevations, wave crests and wave-crest groups under oceanic conditions (Socquet-Juglard et al. 2005; Tayfun 2006; Tayfun & Fedele 2007). If this is indeed the case, then the NB model may also be used in approximating the expected 3D spatial configuration of large storm waves, replacing the temporal auto- and cross-correlation kernels with their most general forms $\rho = \langle \eta(t_0 + \tau, \boldsymbol{x} + \boldsymbol{X}) \, \eta(t_0, \boldsymbol{x}) \rangle$ and $\hat{\rho} = \langle \eta(t_0 + \tau, \boldsymbol{x} + \boldsymbol{X}) \, \hat{\eta}(t_0, \boldsymbol{x}) \rangle$, with $\boldsymbol{x} = (x, y)$ and $\boldsymbol{X} = (X, Y)$. An additional modification required for the NB-theory to predict the expected shape of the largest of *N* waves in 3D wave fields is that instead of Eq. (7b), the latter statistic assumes the form (Socquet-Juglard et al. 2005)

$$\langle Y_N \rangle \cong y_N + \frac{\mu}{2} y_N^2 + \frac{0.577216\,(1 + \mu\, y_N)}{y_N - (1/\, y_N)} \quad , \qquad (31a)$$

where

$$y_N = \sqrt{2 \ln N + \ln (2 \ln N + \ln(\, 2 \ln N + \cdots))} \,. \qquad (31b)$$

Theoretically, QD 2 has wider range of applicability for long- and short-crested waves in deep and transitional water depths. In particular, given the directional spectral density, the expected structure of large waves, and the evolution of their groups in 3D spatial fields are described by Eq. (24), including the spatial variables $\boldsymbol{x}$ and $\boldsymbol{X}$ in the definitions ρ and λ , and defining $\langle Y_N \rangle$ via Eqs. (31a) and (31b) as for the NB model.

COMPARISONS

Of the two data sets to be analyzed here, the first comprises 9-h continuous measurements gathered at 5.12 Hz during a severe storm in January, 1993 with a Marex radar from the Tern platform in the northern North Sea in 167 m water depth. This data will hereafter be referred to as TERN 93. The second set represents 4.5-h measurements gathered at 4 Hz as part of the

Wave Crest Sensor Intercomparison Study (WACSIS) in January, 1998 with a Baylor wave staff from Meetpost Noordwijk in 18 m average water depth in the southern North Sea. TERN 93 is an extremely severe, but fairly stationary deep-water sea state. The WACSIS data set is also fairly stationary, but more typical of a transitional water depth situation.

The analyses of both data for zero-up crossing waves were based on ½-h segments scaled by the corresponding *rms* values. This process gives 3157 zero-up-crossing waves for TERN 93 and 2389 for WACSIS. In the comparisons below, the observed profiles of the maximum waves measured in both cases, the average profiles of 1% highest waves in TERN 93 and 10% highest waves in WACSIS are compared with the QD 1, QD 2, J and NB model predictions. Obviously, the maximum profiles are random in contrast with the theoretical predictions.

The results for the largest wave of TERN 93 are shown in Fig. 2. The comparisons between the average profile of 1% highest waves in TERN 93 and model predictions are in Fig. 3, where the model predictions use the observed statistics, including the NB model (NB-data). The same profile is repeated in Fig. 4 again, comparing it in this case with NB-data and NB-theory based on the theoretical statistics for μ =0.096 and n =100 corresponding to 1% highest waves. In all three figures, the second-order models do compare reasonably well with the observed data and evidently better than the linear QD 1 predictions. Further, all model predictions appear fairly close for the most part, with J doing possibly somewhat better than QD 2 and NB in representing the sharper slopes along the central wave crest. The NB-theory and NB-data predictions, and the observed and predicted parameters in Fig. 4 also compare quite favorably.

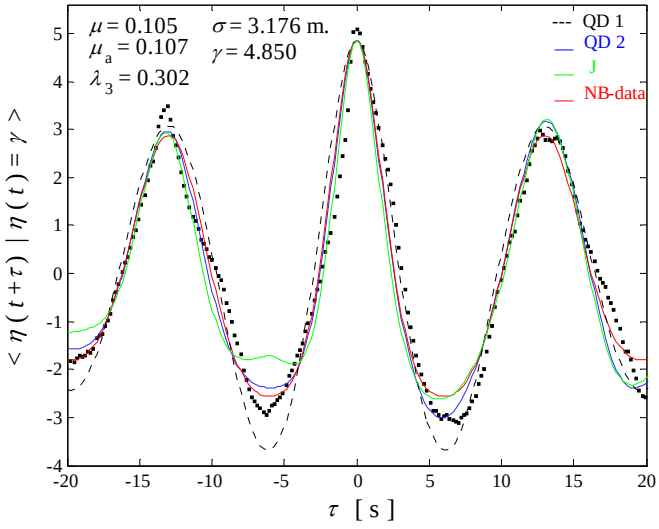

Fig. 2. TERN 93: largest wave (•) vs. model predictions derived from a 30-min series symmetrical about $\gamma = \eta_{\max} = 4.85$.

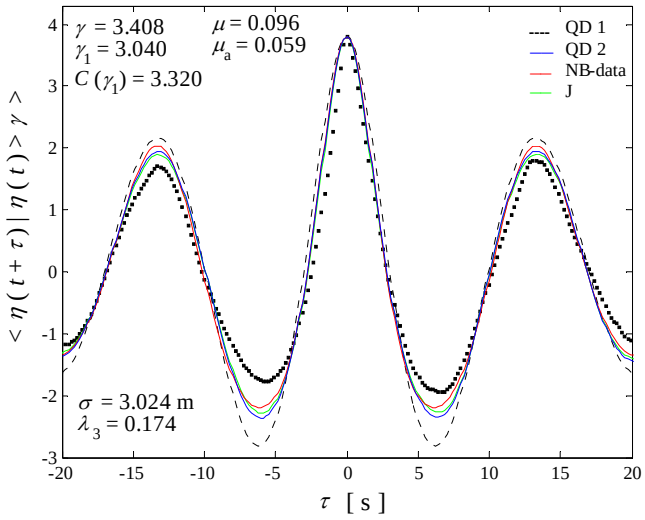

Fig. 3. TERN 93: average profile (•) of 1% highest waves observed vs. model predictions based on observed statistics.

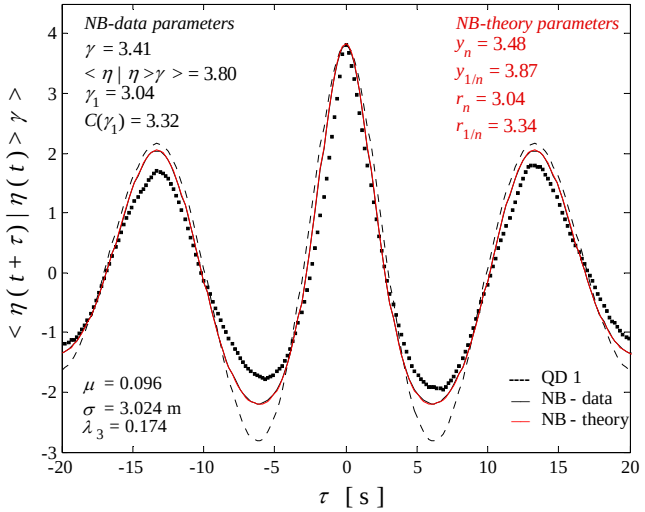

Fig. 4. TERN 93: average profile (•) of 1% highest waves observed vs. model predictions based on theoretical statistics.

The profile of the maximum wave and the expected profile of the 10% largest waves observed in WACSIS versus model predictions are shown in Figs. 5 and 6, respectively, and with the latter case repeated in Fig. 7 to show the comparison between the predictions from NB-data and NB-theory. The overall nature of the WACSIS results is similar to that of TERN 93, except for the somewhat irregular and asymmetric profile of the maximum wave in Fig. 5.

Finally, the profile of the largest wave in TERN 93 is repeated in Fig. 8 in a comparison with the theoretically

expected profile of the maximum of 3,157 waves implied by the QD 1, NB and QD 2 models. As an additional and somewhat extreme example, the theoretically expected profiles for the largest in N=10^5 hypothetical waves representative of TERN 93 are shown in Fig. 9, as predicted with the NB, QD 1 and QD 2 models. There are obviously no such waves actually observed during the TERN measurements, and the predicted profiles suggest the possibility that such waves could have been observed, e.g. had the measurements continued much longer and/or if many simultaneous gauges had been used for measuring about 10^5 waves altogether.

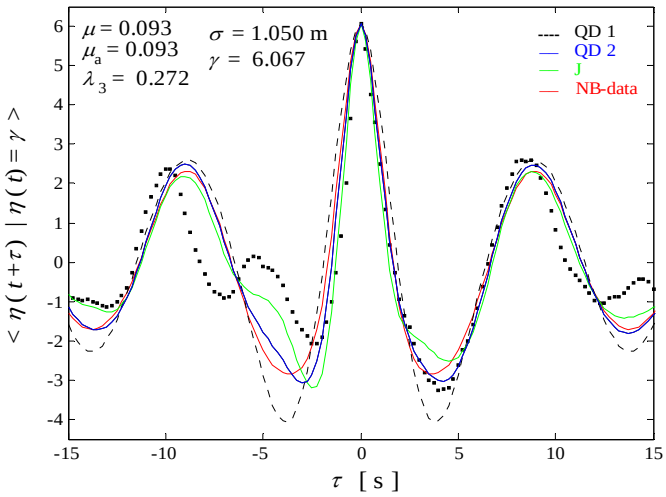

Fig. 5. WACSIS: largest wave (•) vs. model predictions derived from a 30-min series symmetrical about $\gamma = \eta_{max} \cong 6.07$.

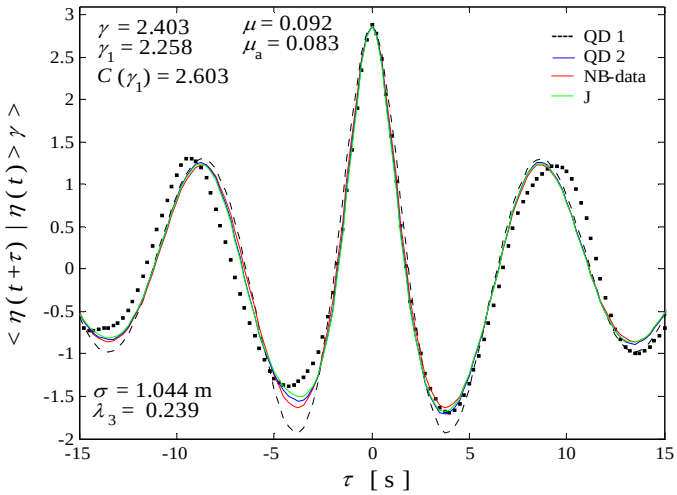

Fig. 6. WACSIS: average profile (•) of 10% highest waves observed vs. model predictions based on observed statistics.

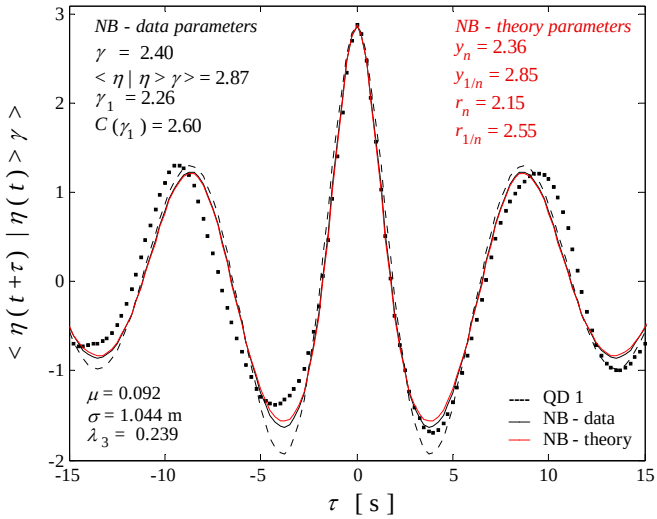

Fig. 7. WACSIS: average profile (•) of 10% highest waves observed vs. model predictions based on theoretical statistics.

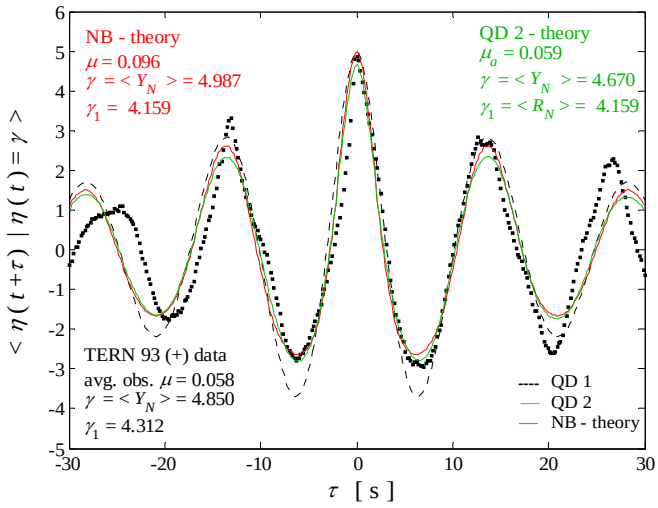

Fig. 8. TERN 93: expected profile of the largest in N = 3,157 waves from model predictions vs. the largest wave actually observed.

CONCLUSIONS

The second-order NB model appears as a simple model well suited for describing and/or predicting the expected shape of large waves, conditional on a variety of possible constraints. The present comparisons of this model and those due to Jensen et al. (1995) and Fedele & Arena (2005) indicate that all three models do reasonably well and certainly far better than any

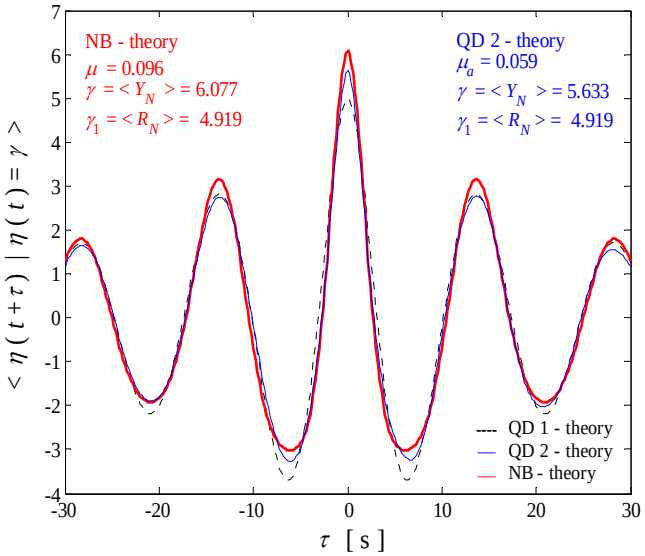

Fig. 9. TERN 93: theoretically expected profile of the largest in $N = 10^5$ waves predicted from NB and QD 2 models.

linear model in representing the profiles of large oceanic waves. Most notably, the quasi-deterministic model of Fedele & Arena (2005) is exact to second-order. Thus, it can be used for describing and/or predicting the expected configuration of large waves in 2D and 3D spatial wave fields in deep or transitional water depths, given the directional spectrum of the sea surface. The same model also lends strong support to the relative validity of the NB model, particularly, in representing the surface elevations, crests and troughs of large waves.

ACKNOWLEDGMENTS

The authors thank G. Z. Forristall, Ocean Engineering, Inc., Camden, ME, USA, for the TERN 93 and WACSIS data.

REFERENCES

Boccotti, P. 2000. *Wave Mechanic for Ocean Engineering*. Elsevier Science, Oxford.

Fedele, F. & Arena, F. 2005. Weakly nonlinear statistics of high random waves. *Phys. Fluids* **17** , paper no. 026601. APS. Germany, paper no OMAE 2006-92527.

Fedele, F. & Tayfun, M. A. 2006. Extreme events and stochastic wave groups. *Proc. OMAE2006*, ASME, Hamburg,

Guedes Soares, C. & Pascoal, R. 2005. On the profile of large ocean waves. *J. of Offshore Mech. & Arctic Eng.* **127**, 306-314.

Jensen, J.J. 1996. Second-order wave kinematics conditional on a given wave crest. *Applied Ocean Res.* **18**, 119-128.

Jensen, J.J., Baatrup, J. & Mansour, A.E. 1995. A conditional second-order wave theory. *Proc. OMAE'95*, ASME, Copenhagen, Denmark, Vol. **IA**, 347-355.

Jensen, J.J. 2005. Conditional second-order short-crested water waves applied to extreme wave episodes. *J. Fluid Mech.* **545**, 29-40.

Lindgren, G. 1972. Local maxima of Gaussian fields. *Arkiv för Matematik* **10**, 195-218.

Petrova, P., Z. Cherneva, Z. & Guedes Soares, C. 2006. On the adequacy of second-order models to predict abnormal waves. *Ocean Engineering*, in press.

Phillips, O. M., Gu, D. & Donelan, M. 1993. Expected structure of extreme waves in a Gaussian sea. Part I: theory and SWADE buoy measurements. *J. Phys. Oceanogr.* **23**, AMS, 992-1000.

Sharma, J. & Dean, R.G. 1979. Second-order directional seas and associated wave forces. *Proc. Offshore Technology Conference*, paper 3645, 2505-2514.

Socquet-Juglard, H., Dysthe, K., Trulsen, K., Krogstad, H. E. & Liu, J. 2005. Probability distributions of surface gravity waves during spectral changes. *J. Fluid Mech.* **542**, 195-216.

Tayfun, M. A. 1980. Narrow-band nonlinear sea waves. *J. Geophys. Res.* **85** (C12), AGU, 1548-1552.

Tayfun, M.A. 1986. On narrow-band representation of ocean waves 1. theory. *J. Geophys. Res.* **91** (C6), AGU, 7743-7752.

Tayfun, M.A. 2004. Statistics of wave crests in storms. *J. Waetrway., Port, Coasal. & Ocean Engineering* **130** (4), ASCE , 155-161.

Tayfun, M. A. 2006. Statistics of nonlinear wave crests and groups. *Ocean Eng*ineering **33**, Elsevier Science, 1589-1622.

Tayfun, M.A. & Fedele, F. 2006. Wave height distributions and nonlinear effects. *Proc. OMAE2006*, ASME, Hamburg, Germany, paper no. OMAE2006-92019.

Tayfun, M.A. & Fedele, F. 2007. Wave height distributions and nonlinear effects. *Ocean Engineering*, Elsevier Science, in press.